CONEM 2016 CONGRESSO NACIONAL DE ENGENHARIA MECÂNICA
21 - 25 AGOSTO DE 2016 FORTALEZA - CEARÁ

PRESSURE DROP CALCULATION FOR SINGLE PHASE LIQUID FLOWS IN RECTANGULAR BIFURCATED MICROCHANNELS

Mila Rosendahl Avelino[1,2], Mila.Avelino@pq.CNPq.br
Jordana Colman[3], jordanacolman@yahoo.com.br
Flávio Peres Amado[1], fpamado@live.estacio.br
[1]Universidade Estácio de Sá – UNESA, R. Eduardo Luiz Gomes, 134 - Morro do Estado, Niterói - RJ, 24020-340.
[2]Universidade do Estado do Rio de Janeiro – UERJ, R. Fonseca Téles, 121 - Rio de Janeiro - RJ, 20940-200
[3]Universidade Federal do Rio de Janeiro, UFRJ, Universidade Federal do Rio de Janeiro, UFRJ Cx. Postal 68503, Cidade Universitária, 21945-970, Rio de Janeiro, RJ, Brazil

Resumo: *The use of bifurcated microchannel flow passages is becoming more common in a number of industrial applications including bioengineering and oil industry. Flow behavior in geometries with small diameter passages is well documented and often relied upon in a practical system. The present work focuses on the flow of single-phase liquids in bifurcated microchannel passages. The compressibility effects, slip boundary condition, and the rarefied flow concerns do not apply for these single-phase liquid flows in microchannels. For the present work, it is assumed that the continuum assumption is valid for microchannels larger than 1.0 μm in hydraulic diameter, however, when considering pressure drop in a microchannel flow it is required to consider its explicit dependence on the hydraulic resistance. The present work evaluates pressure drop for single phase liquid flows in rectangular bifurcated microchannels, taking into account the explicit dependence on the hydraulic resistance. Hydraulic diameter and pressure drop estimation for the bifurcated microchannels are in agreement with the experimental results obtained. It is concluded that the conventional Stokes and Poiseuille flow theories apply for single-phase liquid flow in microchannel.*

Palavras-chave: *microfluidics, pressure drop, microchannels*

1. INTRODUÇÃO

The use of microchannel flow of a fluid confined in a microchannel is becoming more common in a number of industrial applications. Understanding the associated phenomena in order to improve the heat transfer and mass transfer coefficients has motivated the proposal of many techniques, such as extended surfaces, treated surfaces, mechanical aids, and flow devices from the small diameter passages. Recent literature documents well the techniques, and often relied upon in a practical system. (Zhang, 2015, 2016, Attalla et alli 2016, Barisik and Beskok 2016, Heshmati and Ertürk 2016, Liakopoulos, et al., 2016, Manay e Sahin, 2016)

Therefore, it is important to predict flowing properties of a confined fluid in a microchannel. Molecular dynamic simulation (MDS) has been used to analyze velocity profiles and the influence of the wall, allowing to predict shear stress and thus, determine pressure drop occurring in a microchannels.

Fluid mechanics regimen has been reinvestigated by the scientific community in order to better understand the behavior of the fluid near the wall in the new dimensions. Steinke et al (2005).

Bridges between the classical theory and the theory at different scales has been a real challenge for engineers and also for the scientific community. For the present work, it will be assumed that the continuum assumption is valid for microchannels larger than 1.0 μm in hydraulic diameter.

The present work focuses on the flow of single-phase liquids in microchannel passages. The compressibility effects, slip boundary condition, and the rarefied flow concerns do not apply for these single-phase liquid flows in microchannels. For the present work, it will be assumed that the continuum assumption is valid for microchannels larger than 1.0 μm in hydraulic diameter.

2. PRESSURE DROP

2.1. Friction factor Fundamentals

According to Steinke and Kandlikar (2005), the starting point in the theoretical discussion will be the definition of friction factor, f. One complication for determining the friction factor is the two different definitions for f, Darcy and Fanning. The Fanning definition of friction factor will be utilized, as in Kandlikar at alli (2005), because it is more convenient when performing adiabatic experiments. It takes the same form of the Colburn *j* factor equation. Therefore, a link between the heat transfer performance and the pressure drop performance is made through the f and j factors. The Fanning friction factor is defined as the ratio of the wall shear stress to the flow kinetic energy per unit volume and is found using Eq. (1).

$$f = \frac{\tau_w}{\left(\frac{1}{2}\right)\rho V^2} \ , \tag{1}$$

where f is the Fanning friction factor, τ_w is the wall shear stress, ρ is the fluid density, and V is the average velocity. The friction factor in terms of the pressure drop and mass flux is given by Eq.(2). In considering the pressure drop of a flow confined to a microchannel it is necessary to consider its dependence on the hydraulic resistance. Eq. (2), takes into account the explicit dependency of the hydraulic resistance on the pressure gradient, by definition, (Steinke and Kandlikar, 2005),

$$f = \frac{\rho \Delta p D_h}{2 L G^2} \ , \tag{2}$$

where Δp is the pressure drop, D_h is the hydraulic diameter, L is the passage length, and G is the mass flux.

The Poiseuille number is a function of aspect ratio for a rectangular passage. It can be determined using Eq. (3) from Shah and London (1978).

$$f \ \mathrm{Re} = 24(1.3553\alpha c + 1.9467\alpha c^2 - 1.7012\alpha c^3 + 0.9564\alpha c) \ , \tag{3}$$

where αc is the channel aspect ratio. One constraint for this equation is that the aspect ratio must be less than one. If the channel aspect ratio is greater than 1.0, the inverse is taken to use with Eq. (3).

The turbulent regime has several possible correlations to choose from. Blasius for the smooth round tube correlation is shown in Eq. (4). Steinke and Kandlikar (2005).

$$f = \frac{0.0791}{\mathrm{Re}^{1/4}} \ . \tag{4}$$

This correlation is valid for the range of 2, 100 < Re < 105 and for e/D ratios < 1×10−6.The pioneering work of Nikuradse (1933) varied the roughness of pipes using sand adhered to the walls using a lacquer. He determined the dependence of friction factor upon a nondimensional wall roughness as seen in Eq. (5).

$$\frac{1}{\sqrt{f}} = 3.48 - 1.737 \ln\left(\frac{e}{D}\right) , \tag{5}$$

for e/D ratios > 1×10−6, the friction factor can also be determined by using the implicit Colebrook (1938–1939) equation shown in Eq. (6).

$$\frac{1}{\sqrt{f}} = 3.48 - 1.737 \ln\left(\frac{e}{D} + \frac{9.35}{\mathrm{Re}\sqrt{f}}\right) . \tag{6}$$

According to Steinke and Kandlikar (2005) correlation is widely accepted as the basis for the turbulent region in the Moody (1944) diagram. The property ratio method for viscosity given in Kakaç et al. (1987) is given in Eq. (7)

$$\frac{f}{f_{cp}} = \left(\frac{\mu b}{\mu w}\right) m \ , \tag{7}$$

where f_{cp} is the constant property friction factor, f is the property corrected friction factor, μb is the viscosity of the fluid calculated at the bulk fluid temperature, μw is the viscosity of the fluid calculated at the wall temperature, and m=−0.58 for laminar heating in a fully developed, circular duct.

2.2. Hydrodynamically developing flow

The hydrodynamically developing flow can become quite important in microchannels. Steinke and Kandlikar (2005). Due to the often short lengths, the developing flow could dominate the entire flow length of the microchannel. First, the definition of a non-dimensional flow distance is defined in Eq. (8).

$$x^{+} = \frac{x}{D_h Re} \tag{8}$$

where x + is the non-dimensional flow distance and x is the axial flow direction location. It is commonly accepted that for a value of x+ = 0.05, the flow can be considered fully developed. When considering the developing flows, the pressure drop is now related to an apparent friction factor and is seen in Eq. (11), Kakaç et al. (1987).

$$\Delta p = \frac{2\left(f_{app} Re\right)\mu V_x}{D_h} \tag{9}$$

where f_{app} is the apparent friction factor, μ is the viscosity, and x is the axial location of interest. If the entire length of the microchannel is considered, the x term can be the microchannel length. According to Steinke and Kandlikar (2005) the apparent friction factor consists of two components. The first is the friction factor from the theory for the fully developed flow and the second is the pressure defect (a.k.a. Hagenbach factor) as given by Eq. (12).

$$\Delta p = \frac{2\left(f_{app} Re\right)\mu V_x}{D_h} + \frac{k(x)\rho V^2}{2} \tag{12}$$

where κ is the Hagenbach factor given by Eq (13)

$$k(x) = \left(f_{app} - f_{FD}\right)\frac{4x}{D_h} \tag{13}$$

The Hagenbach factor will begin at a value of 0 and increase to some fully developed constant value k(∞). Hagenbach factor has a dependence upon channel aspect ratio for rectangular channels. Eq. (14), with an accuracy of 0.04%, determines the fully developed Hagenbach factor for a rectangular channel.

$$k(\infty) = \left(0.6796 + 1.2197\ \alpha_c{}^{1} + 3.3089\ \alpha_c{}^{2} - 9.5921\ \alpha_c{}^{3} + 8.9089\ \alpha_c{}^{4} - 2.9959\ \alpha_c{}^{5}\right) \tag{14}$$

2.3. Pressure drop measurements in microchannel flows

According to Steinke and Kandlikar (2005) there are several issues that need to be addressed when performing pressure drop measurements in microchannel flows. Generally, there are three main components that contribute to the overall pressure drop. The inlet and exit losses need to be quantified for the microchannel. The hydrodynamic developing length needs to be carefully evaluated. Finally, the remaining length will have the fully developed frictional loss.

In fact, in a flow gradient of zero pressure, i.e., loss of constant load, the flow will also be constant. This result is in accordance with the law of Hagen- Poiseulle, Equations 8 and 9.

$$R_{hidrl}\left(\Delta p\right) \equiv \frac{\Delta p}{Q_{mass}\left(\Delta p\right)} \tag{8}$$

$$\Delta p = R_{hidrl}\ Q = \frac{1}{G_{hidrl}} Q \qquad (9)$$

where Rhidrl e Ghidrl are proportionality factors known to hydraulic conductance and resistance, respectively. The Hagen -Poiseuille law is analogous to Ohm's law (DV = RI) , relating to electric current I with the electrical resistance R and DV potential difference . The electrical analogy will be used later for the pressure loss calculation in the flow.

The microdevice studied was a separation device as shown in Figure 1, the entrance has 10.30mm length, 400 µm width and depth of 50 µm, with a lager junction with geometry length of 9.0mm , a width of 400 µm and depth of 50 µm and the thinner channel 9.0mm long, width of 100 µm and 50 µm depth . Input flow value was 0.017mL.

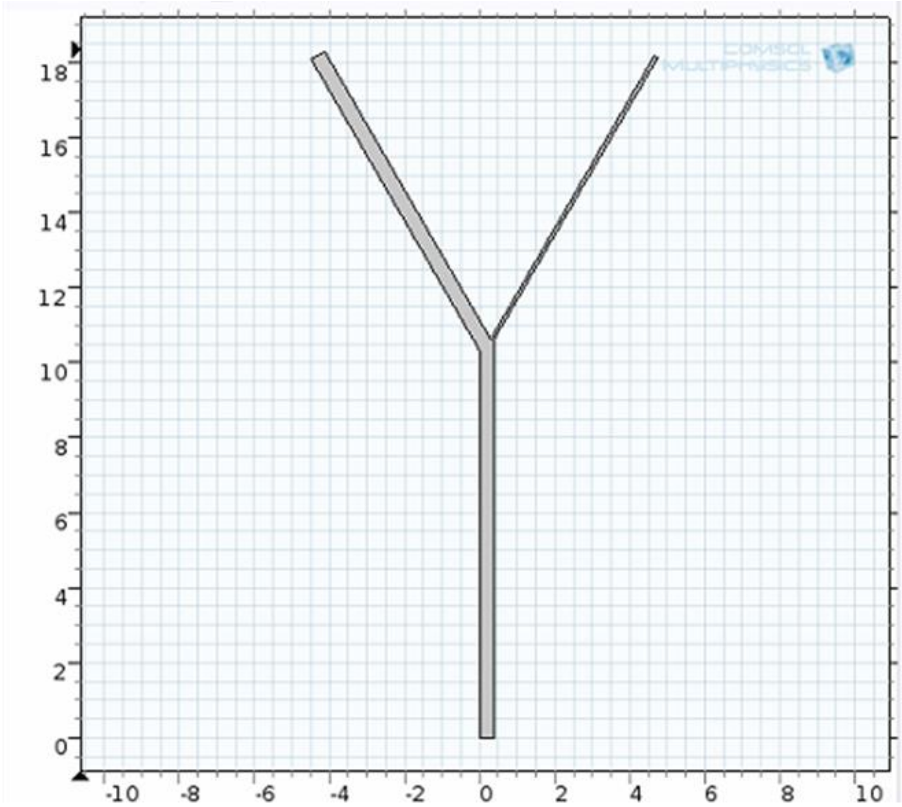

Figure 1: Microdevice with bifurcation.

The values of hydraulic resistance, hydraulic diameter, velocity and Reynolds number obtained through an analogy with the circuit are shown in Table 1.

Table 1. hydraulic resistance , hydraulic diameter, velocity and Reynolds number for the studied microchannel.

Microchannel	width (µm)	lenght (mm)	hight (µm)	Q (ml/min)	D_H (µm)	$R_{Hidrod.}$ (Pa.s/m³)	V (m/s)	Re
In	400	10,30	50	0,0166	88,89	$2.39.10^{12}$	0,0139	1,232
Out larger	400	9,0	50	0,0146	88,89	$2.08.10^{12}$	0,0121	1,072
Out thiner	100	9,0	50	0,0020	66,67	$1.12.10^{13}$	0,0068	0,452

The phenomenon of influence of the pressure gradient in determining the hydraulic resistance is critical to the microchannel design.

Likewise, the electrical resistance is related to the dissipation of energy by Joule effect, the hydraulic resistance due to the viscous dissipation of mechanical energy resulting from friction of the fluid.

The behavior of the energy dissipation due to viscous effects in the Poiseuille flow is analogous to the behavior of the electric power consumed by the Joule effect, so the electrical analogy introduced as appropriate tool for estimating the fluid resistance.

3. MICROCHANNELS OF CONSTANT RECTANGULAR CROSS SECTION

To ensure that the law of the bifurcation is applied, the hydraulic diameter of the outlet channels may not be equal. Thus, 3 different widths to output channels have been proposed, 80µm and 100µm 200µm. Figure 2 shows the projected separator microdevice : the separator microdevice 1 with input 400µm wide and one of equal diameter outlet channels (bifurcation most left side) and the other output channel 80µm (split lower right side), the separator microdevice 2 with input 400µm wide and one of equal diameter outlet channels (bifurcation most left side) and the other output channel 100µm (split lower right side), the separator microdevice 3 with 400µm wide input and a of equal diameter outlet channels (bifurcation most left side) and the other 200µm output channel with equal time among all of 50µm (split lower right side).

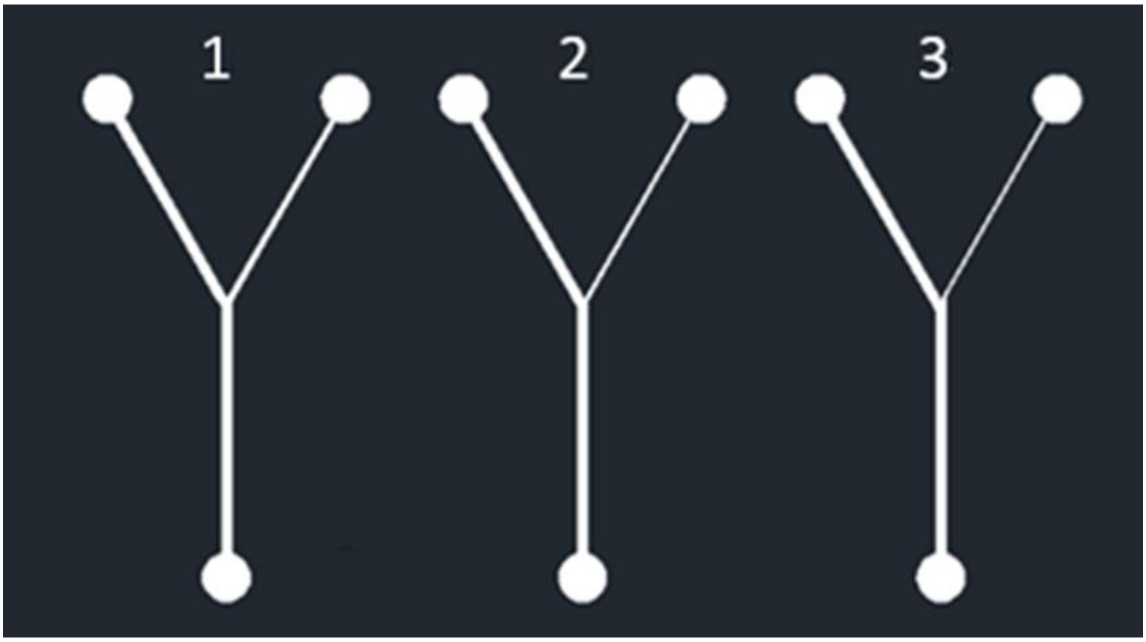

Figure 2. Separation Microdevice Proposed In This Paper

Table 2 summarizes analyzed and manufactured microfluidic geometries shown in Figure 3.4, such as length, width and height of 50µm. These geometries are different because we attempted to see if could even equal lengths and different widths, applying the law of the fork, resulting in non- utilization of Separation Microdevice 1 and 3 for the study.

Table 3 : Width fixed for microdevices shown in Figure 2, with the fixed length and calculated by hydraulic resistance , with a height of 50µm .

	Analised						Manufactured		
microsseparators	WIDTH (μm)			LENGHT (mm)			LENGHT (mm)		
	In	Bif. larger	Bif. smaller	In	Bif. larger	Bif. smaller	In	Bif. larger	Bif. smaller
Micr. 1 - 200μm	400	400	200	10,3	9,0	22,0	10,3	9,0	9,0
Micr. 2 - 100μm	400	400	100	10,3	9,0	9,0	10,3	9,0	9,0

Micr. 3 - 80μm	400	400	80	10,3	9,0	6,4	10,3	9,0	9,0

In Table 3, we can see that the ratio of the flow rates of microdevices analyzed by analogy as electric circuit, has reason above, thus fulfilling the law of bifurcation , since the microdevices presented in Table 4 which were manufactured with the same fork lengths , only microdevices 2 shows a satisfactory ratio between the flow of outgoing junctions , as this may only be used in the present study .

Table 4: Expected values for length, diameter hydraulic, fluid resistance, flow, width and height of 50μm, for the analyzed microdevices, shown in Figure 2.

Microdevices	**Dh (μm)**			**Rhidr (kg/m⁴.s)**			**Flow rate(ml/min)**			**Velocity (m/s)**			**Re**		
	In	Bif. Maior	Bif. Menor	In	Bif. Maior	Bif. Menor	In	Bif. Maior	Bif. Menor	In	Bif. Maior	Bif. Menor	In	Bif. Maior	Bif. Menor
Micr. 1 - 200μm	88,89	88,89	66,67	2,39.10^{12}	2,08.10^{12}	1,12.10^{13}	0,017	0,014	0,02	0,0139	0,012	0,004	1,23	1,06	0,27
Micr. 2 - 100μm	88,89	88,89	66,67	2,39.10^{12}	2,08.10^{12}	1,12.10^{13}	0,017	0,014	0,002	0,0139	0,012	0,007	1,23	1,06	0,27
Micr. 3 - 80μm	88,89	88,89	66,67	2,39.10^{12}	2,08.10^{12}	1,12.10^{13}	0,017	0,015	0,002	0,0139	0,013	0,004	1,23	1,06	0,27

Table 5: Values width , length, diameter hydraulic , hydraulic resistance , flow and height of 50μm to microdevices manufactured , shown in Figure 3.4.

Microsseparadores	**Diâmetro hidráulico (μm)**			**Resistência hidráulica (kg/m⁴.s)**			**Vazão (ml/min)**			**Velocidade (m/s)**			**Re**		
	Entrada	Bif. Maior	Bif. Menor	Entrada	Bif. Maior	Bif. Menor	Entrada	Bif. Maior	Bif. menor	Entrada	Bif. Maior	Bif. Menor	Entrada	Bif. Maior	Bif. Menor
Micr. 1 - 200μm	88,89	88,89	66,67	2,39.10^{12}	2,08.10^{12}	4,56.10^{12}	0,017	0,008	0,008	0,0139	0,009	0,008	1,23	0,79	0,53
Micr. 2 - 100μm	88,89	88,89	66,67	2,39.10^{12}	2,08.10^{12}	1,12.10^{13}	0,017	0,014	0,002	0,0139	0,012	0,007	1,23	1,06	0,27
Micr. 3 - 80μm	88,89	88,89	66,67	2,39.10^{12}	2,08.10^{12}	1,57.10^{13}	0,017	0,002	0,014	0,0139	0,013	0,006	1,23	1,15	0,40

Given the proposed geometry, the hydraulic diameter was calculated and established an inlet flow value of 0.017ml/min, the length of the input channel and one output channel through the hydraulic resistance of each of the microdevice was calculated optimum length of the smaller hydraulic diameter exit channel (Table 3).

It was then offered a 10.30mm microdevices with an input length and an output length equal bifurcations in both 9mm and three different widths (Table 2). As can be seen in Table 3, the flow between the output channels of 200μm and 80μm are not in accordance with the law of bifurcation, and thus rendered useless for the study because its flow in the smallest channel is equal to the largest channel or higher confirming so that its length would have to be differentiated. Based on the calculations presented in Table 3.3, the microdevices having the law of the fork and with different hydraulic diameters and hydraulic resistance values of microdevices 2, which has input 10.30mm and 400μm wide, 9mm one of outputs and 400 mm in width and lower output value 9mm in length and 100μm in width with a height of 50μm homogeneously throughout the microdevices.

4. EXPERIMENTAL RESULTS FOR PRESSURE DISTRIBUITIONS

The Figure 3 presents the pressure distribution calculated for the points within the microchannels.

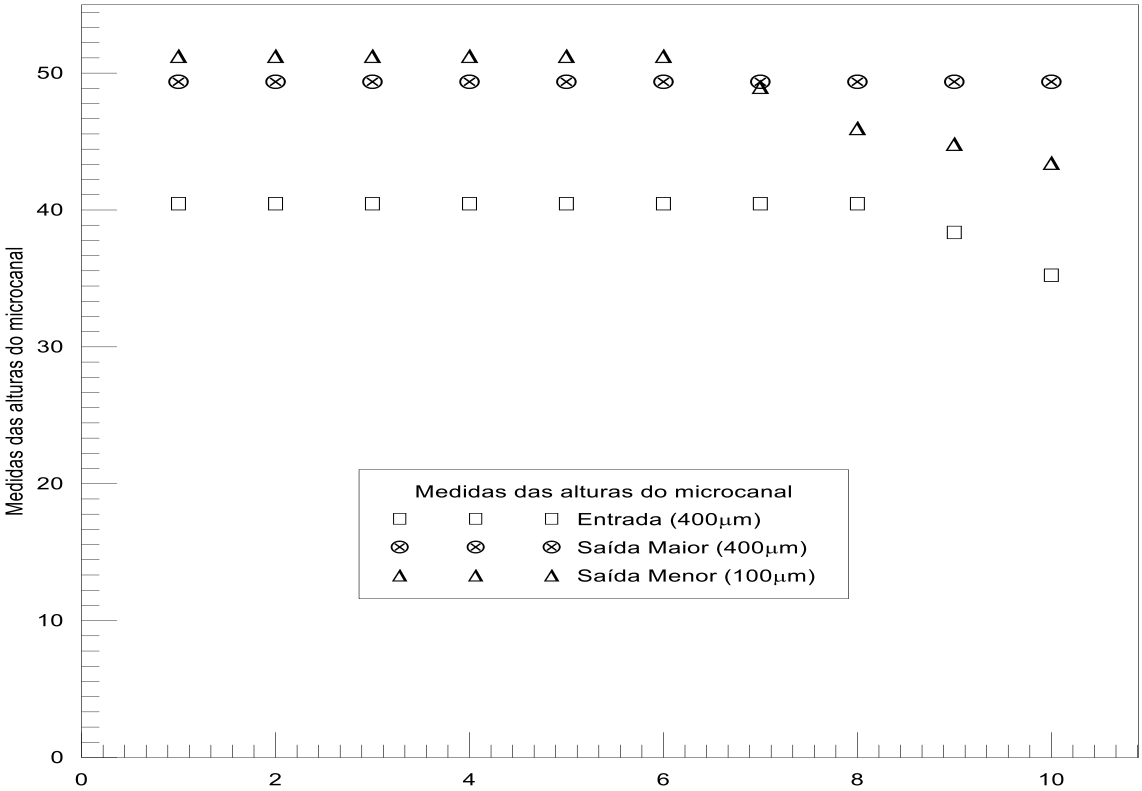

Figure 3. Results for pressure drop calculation obtained with the proposed model..

5. NUMERICAL RESULTS FOR PRESSURE DISTRIBUITIONS

Simulations in finite difference method and through the commercial code were made for determine velocity profiles and pressure gradients.

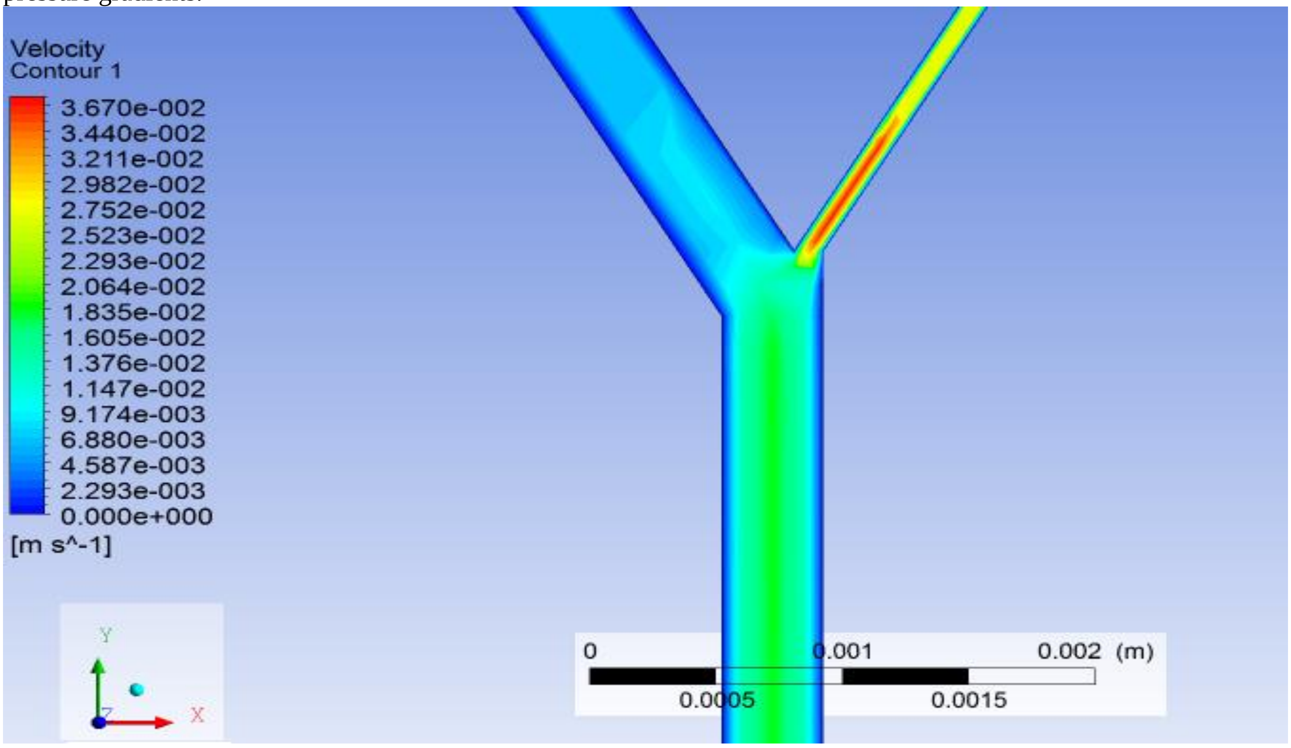

Figure 4: Velocity profile

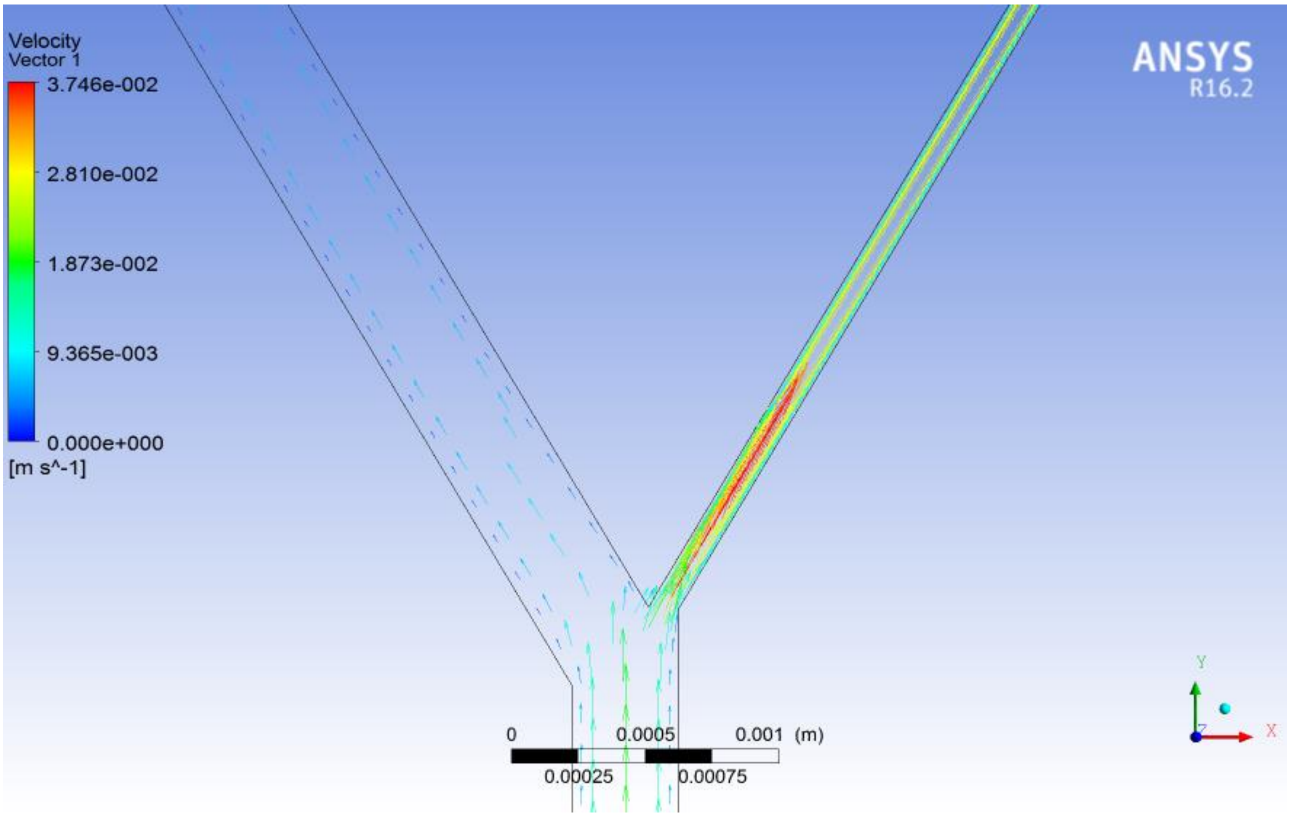

Figure 5: Velocity profile

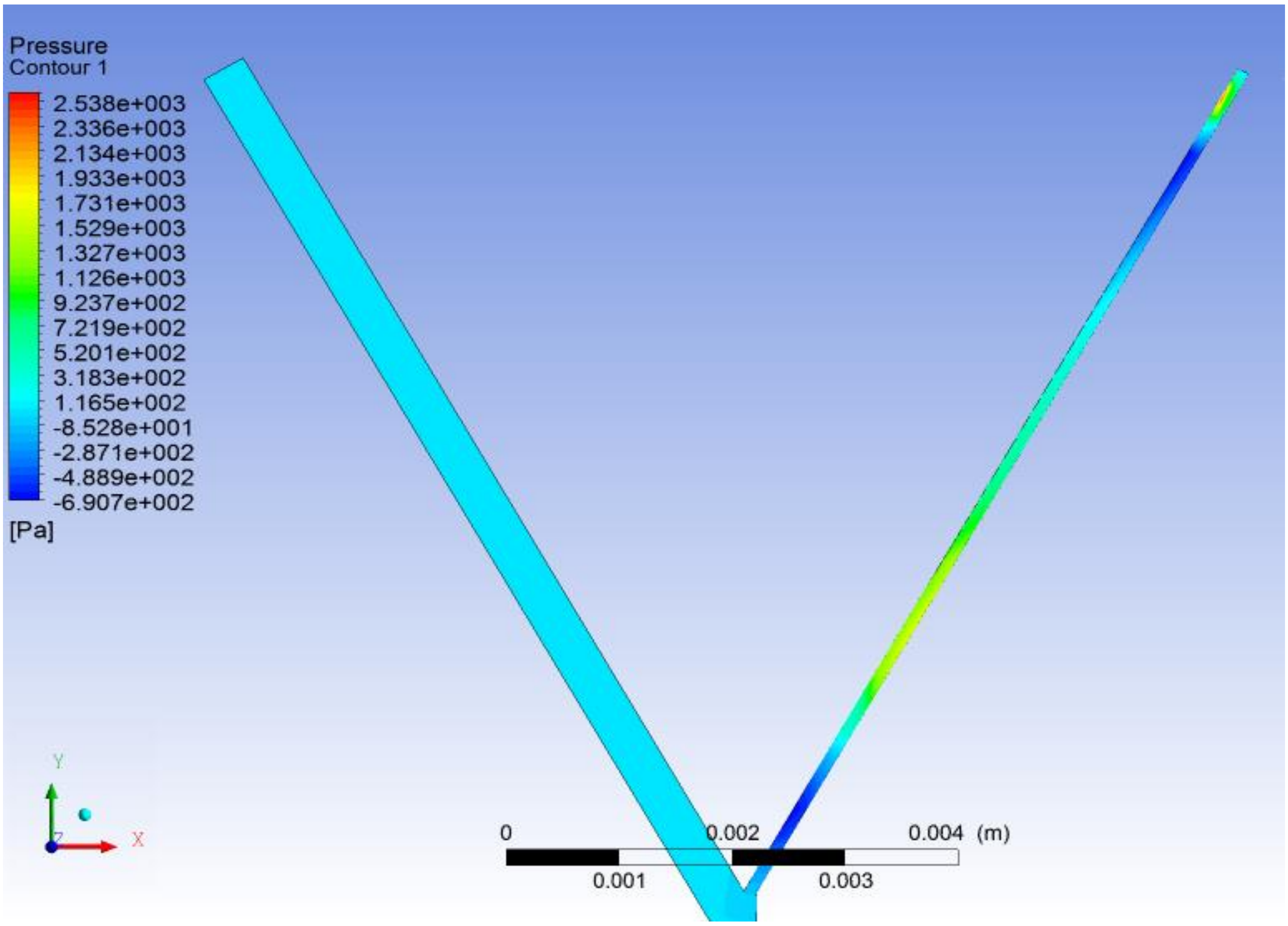

Figure 6: Velocity profile

6. CONCLUSIONS

The present work shows that classical theory for pressure drop calculations for flow of single-phase liquids in channel passages cam be used to predict similar geometries in microchannels. The compressibility effects, slip boundary condition, and the rarefied flow concerns do not apply for these single-phase liquid flows in microchannels. For the present work, it was assumed that the continuum assumption is valid for microchannels larger than 1.0 µm in hydraulic diameter, and is was proved to be reasonable.

7. ACKNOWLEDGMENTS

The authors acknowledge “Programa Pesquisa Produtividade” - Universidade Estácio de Sá for funding this research.

8. REFERÊNCIAS

AKBARI, Mohsen, David Sinton, and Majid Bahrami. "Pressure drop in rectangular microchannels as compared with theory based on arbitrary cross section." Journal of Fluids Engineering 131.4 (2009): 041202.

ATTALLA, M.; MAGHRABIE, Hussein M.; SPECHT, E. An experimental investigation on fluid flow and heat transfer of rough mini-channel with rectangular cross section. Experimental Thermal and Fluid Science, v. 75, p. 199-210, 2016.

BAHRAMI, M., M. M. Yovanovich, and J. R. Culham. "Pressure drop of fully developed, laminar flow in rough microtubes." Journal of fluids engineering 128.3 (2006): 632-637.

BARISIK, Murat; BESKOK, Ali. “Law of the nano-wall” in nano-channel gas flows. Microfluidics and Nanofluidics, v. 20, n. 3, p. 1-9, 2016.

BRUUS, Henrik. Theoretical microfluidics. 2008.

COLEBROOK, C.F., Turbulent flow in pipes with particular reference to the transition region between the smooth and rough pipe laws, J. Institution of Civil Engineers, London 11 (1938–1939) 133–156.

FEKETE, Zoltán et al. Performance characterization of micromachined particle separation system based on Zweifach–Fung effect. Sensors and Actuators B: Chemical, v. 162, n. 1, p. 89-94, 2012.

HESHMATI, Farid; ERTÜRK, Hakan. Single-phase models for improved estimation of friction factor for laminar nanofluid flow in pipes. International Journal of Heat and Mass Transfer, v. 95, p. 416-425, 2016.

KAKAÇ, S., R.K. Shah, W. Aung, Handbook of Single-Phase Convective Heat Transfer, John Wiley & Sons, New York, 1987.

KANDLIKAR S.G., D. Schmitt, A.L. Carrano, J.B. Taylor, Characterization of surface roughness effects on pressure drop in single-phase flow, Phys. Fluids 17 (10) (2005).

KENNING, D. B. R. et al. Pressure drop and heat transfer characteristics for single-phase developing flow of water in rectangular microchannels. In: Journal of Physics: Conference Series. IOP Publishing, 2012. p. 012085.

KIRBY, Brian J. Micro-and nanoscale fluid mechanics: transport in microfluidic devices. Cambridge University Press, 2010.

LIAKOPOULOS, Antonios; SOFOS, Filippos; KARAKASIDIS, Theodoros E. Friction factor in nanochannel flows. Microfluidics and Nanofluidics, v. 20, n. 1, p. 1-7, 2016.

MANAY, Eyuphan; SAHIN, Bayram. The effect of microchannel height on performance of nanofluids. International Journal of Heat and Mass Transfer, v. 95, p. 307-320, 2016.

MOODY, L.F., Friction factors for pipe flow, Trans. ASME 66 (8) (1944) 671–684.

MUZYCHKA, Y. S., and M. M. Yovanovich. "Pressure drop in laminar developing flow in noncircular ducts: A scaling and modeling approach." Journal of Fluids Engineering 131.11 (2009): 111105.

NIKURADSE J., Strmungsgesetze in rauhen Rohren, V.D.I. Forschungsheft 361 (1933) 1–22.

OH, Kwang W. et al. Design of pressure-driven microfluidic networks using electric circuit analogy. Lab on a Chip, v. 12, n. 3, p. 515-545, 2012.

SAJEESH, P.; SEN, Ashis Kumar. Particle separation and sorting in microfluidic devices: a review. Microfluidics and nanofluidics, v. 17, n. 1, p. 1-52, 2014.

SHAH, Ramesh K.; LONDON, Alexander Louis. Laminar flow forced convection in ducts: a source book for compact heat exchanger analytical data. Academic press, 2014.

SHARP Microfluidics Chapter 10 in CRC MEMS Handbook

STEINKE, Mark E., and Satish G. Kandlikar. "Single-phase liquid friction factors in microchannels." ASME 3rd International Conference on Microchannels and Minichannels. American Society of Mechanical Engineers, 2005.

STEINKE, Mark E.; Kandlikar, Satish G. Single-phase liquid friction factors in microchannels. In: ASME 3rd International Conference on Microchannels and Minichannels. American Society of Mechanical Engineers, 2005. p. 291-302. [39] R.K. Shah, A.L. London, Laminar Flow Forced Convection in Ducts, Adv. Heat Transfer, Supplement 1, Academic Press, New York, 1978.

TENG, Jyh-tong, et al. Fluid dynamics in microchannels. INTECH Open Access Publisher, 2012

TRIPATHI, Siddhartha et al. Performance study of microfluidic devices for blood plasma separation—a designer's perspective. Journal of Micromechanics and Microengineering, v. 25, n. 8, p. 084004, 2015.

ZHANG, Yongbin. The flow equation for a nanoscale fluid flow. International Journal of Heat and Mass Transfer, v. 92, p. 1004-1008, 2016

ZHANG, Yongbin. A quantitative comparison between the flow factor approach model and the molecular dynamics simulation results for the flow of a confined molecularly thin fluid film. Theoretical and Computational Fluid Dynamics, v. 29, n. 3, p. 193-204, 2015.

ZHANG, Yongbin. Calculating the maximum flowing velocity of the Poiseuille flow in a nanochannel by the flow factor approach model. International Communications in Heat and Mass Transfer, v. 73, p. 111-113, 2016.

ZHANG, Yongbin. Poiseuille flow in a nano channel for different wall surface patterns. International Journal of Heat and Mass Transfer, v. 95, p. 243-248, 2016.

9. RESPONSABILIDADE AUTORAL

The authors are the only responsible for the printed material included in this paper.